Metasurfaces Atop Metamaterials: Surface Morphology Induces Linear Dichroism in Gyroid Optical Metamaterials

James A. Dolan, Raphael Dehmel, Angela Demetriadou, Yibei Gu, Ulrich Wiesner, Timothy D. Wilkinson, Ilja Gunkel, Ortwin Hess, Jeremy J. Baumberg, Ullrich Steiner, Matthias Saba, and Bodo D. Wilts*

Optical metamaterials offer the tantalizing possibility of creating extraordinary optical properties through the careful design and arrangement of subwavelength structural units. Gyroid-structured optical metamaterials possess a chiral, cubic, and triply periodic bulk morphology that exhibits a redshifted effective plasma frequency. They also exhibit a strong linear dichroism, the origin of which is not yet understood. Here, the interaction of light with gold gyroid optical metamaterials is studied and a strong correlation between the surface morphology and its linear dichroism is found. The termination of the gyroid surface breaks the cubic symmetry of the bulk lattice and gives rise to the observed wavelength- and polarization-dependent reflection. The results show that light couples into both localized and propagating plasmon modes associated with anisotropic surface protrusions and the gaps between such protrusions. The localized surface modes give rise to the anisotropic optical response, creating the linear dichroism. Simulated reflection spectra are highly sensitive to minute details of these surface terminations, down to the nanometer level, and can be understood with analogy to the optical properties of a 2D anisotropic metasurface atop a 3D isotropic metamaterial. This pronounced sensitivity to the subwavelength surface morphology has significant consequences for both the design and application of optical metamaterials.

Metamaterials are artificially engineered materials whose optical properties are dependent on both the geometry of their structural units and their chemical composition.[1] The ability to design an effective permittivity $\varepsilon_{eff}(\omega)$ and permeability $\mu_{eff}(\omega)$ by careful choice of these subwavelength structural units offers the potential for intriguing applications, such as superlenses and cloaking devices.[2,3] Associated material properties include those otherwise unavailable in nature, such as a negative refractive index and extreme "hyperbolic" optical anisotropy.[4] The observation of these unique properties at optical frequencies, however, requires structural control on the length scale of just a few nanometers. "Top down" techniques are either unable to produce bulk 3D structures (e.g., electron beam lithography[5,6]), or cannot produce such structures on the nanoscale (e.g., direct laser writing[7–9]), with the uniformity and efficiency necessary for a truly macroscopic $\varepsilon_{eff}(\omega)$ and $\mu_{eff}(\omega)$.[10,11]

Dr. J. A. Dolan[+], Dr. R. Dehmel[++], Prof. J. J. Baumberg
Cavendish Laboratory, Department of Physics
University of Cambridge
J.J. Thomson Avenue, Cambridge CB3 0HE, UK

Dr. J. A. Dolan[+], Prof. T. D. Wilkinson
Department of Engineering
University of Cambridge
J.J. Thomson Avenue, Cambridge CB3 0FA, UK

    The ORCID identification number(s) for the author(s) of this article can be found under https://doi.org/10.1002/adma.201803478.

[+]Present address: Institute for Molecular Engineering, Argonne National Laboratory, 9700 S. Cass Avenue, Argonne, IL 60439, USA

[++]Present address: Papierfabrik Louisenthal GmbH, 83701 Gmund a.T., Germany

[+++]Present address: The Dow Chemical Company, 2301 N. Brazosport Blvd., Freeport, TX 77541, USA

Dr. J. A. Dolan[+], Dr. I. Gunkel, Prof. U. Steiner, Dr. B. D. Wilts
Adolphe Merkle Institute
University of Fribourg
Chemin des Verdiers 4, 1700 Fribourg, Switzerland
E-mail: bodo.wilts@unifr.ch

Dr. A. Demetriadou
School of Physics and Astronomy
University of Birmingham
Edgbaston, Birmingham B15 2TT, UK

Dr. Y. Gu[+++], Prof. U. Wiesner
Department of Materials Science and Engineering
Cornell University
214 Bard Hall, Ithaca, NY 14853-1501, USA

Prof. O. Hess, Dr. M. Saba
Department of Physics
Imperial College London
Prince Consort Road, London SW7 2AZ, UK

Alternative "bottom up" approaches overcome these limitations and allow efficient fabrication of otherwise inaccessible 3D nanoscale structures. One successful method employs self-assembling triblock terpolymers, and results in optical metamaterials with a single gyroid morphology.[12–15] The chemical dissimilarity between the different "blocks" of the terpolymer (i.e., the constituent polymer chains) leads to microphase-separation into various morphologies on the nanometer length scale. These morphologies are used as sacrificial templates to fabricate bulk functional nanomaterials. Here, the resulting structures are 3D metamaterials with macroscopic optical properties which emerge directly from the templated network morphology.[12,16]

The single gyroid structure is a chiral, cubic, and triply periodic geometry found in a variety of natural and synthetic self-assembled systems.[17–20] Its unique morphology[17,21,22] imparts a range of optical properties to gyroid-structured optical metamaterials that are dependent on the unit cell size, volume fill fraction, surrounding refractive index, and degree of order.[12–15,20,23] Intriguingly, gyroid optical metamaterials give rise to a linear and circular dichroism (i.e., a variation in the optical properties as a function of azimuthal orientation of linearly polarized light and handedness of circularly polarized light, respectively), both of which are sensitive to the structure of the metamaterial.[12,13] However, this optical anisotropy is only readily observable (e.g., by standard optical microscopy techniques) when the metamaterial possesses long-range order, whereby domains of the self-assembled template span at least tens of micrometers. If the metamaterial possesses only short-range order, its anisotropic optical properties are masked and it responds similarly to disordered nanoporous gold.[15]

Here, we fabricated and characterized exceptionally large domains of a gold gyroid optical metamaterial and studied their reflectance under various polarizations of incident light. These domains were manufactured from a self-assembled triblock terpolymer template. Since the terpolymer partially crystallizes during solvent vapor annealing, giving rise to a contrast in polarized light microscopy, it is possible to optimize the annealing process to produce polymeric templates with gyroid domains which span hundreds of micrometers.[24]

Previous work has shown that gyroid optical metamaterials exhibit linear dichroism (quantified by a shift of the extinction peak, or change in reflectance, as a function of relative orientation of the gyroid structure and polarization axis of the incident light),[12,13] which is unexpected due to the gyroid's cubic symmetry. Indeed, linear dichroism is absent, by any metric, in all theoretical models of gyroid metamaterials.[23,25–27] To resolve this apparent discrepancy between experiment and theory, and to further study the more general phenomenon of how light couples into periodic network-structured optical metamaterials, we have combined experiments and simulations to demonstrate the effect of the gyroid surface termination, thereby shedding light on the origin of the linear dichroism in gyroid optical metamaterials.

Scanning electron microscopy (SEM) and polarized optical microscopy images in **Figure 1** confirm the successful fabrication of a gold gyroid optical metamaterial with long-range order. The SEM image in Figure 1a reveals an arrangement and symmetry of pores which are consistent with a gyroid morphology oriented with the ⟨110⟩ direction normal to the substrate.[20,28] This is also consistent with previous results using the same and similar triblock terpolymers under identical and near-identical fabrication conditions, which were additionally characterized by (grazing-incidence) small-angle X-ray scattering (SAXS).[24,28] Linearly polarized optical microscopy (Figure 1b) reveals domains randomly oriented in-plane with lateral sizes of ≈50–200 μm, where the color and intensity contrast arises from the linear dichroism of the gyroid metamaterial.[12]

The reflectance spectra of single domains of gyroid optical metamaterials were acquired under linearly polarized light (Figure 1c,d; for a plot on a linear scale see Figure S1 in the Supporting Information). The spectra clearly depend on the azimuthal angle of the incident light φ, showing a strong linear dichroism. As φ increases from 0° to 180°, the reflectance of the metamaterial oscillates around a minimum at 0° ($\lambda \gtrsim 600$ nm); at shorter wavelengths the minimum reflectance is found at slightly larger φ (Figure 1c), hence the mismatch between the 45° and 135° spectra in Figure 1d. The azimuthal angles are defined relative to the in-plane $[\bar{1}10]$ direction of the gyroid, the orientation of maximum reflectance at long wavelengths. Figure S2 shows the equivalent transmittance data, which is complementary to the reflectance data of Figure 1c,d and similarly exhibits a strong linear dichroism. The same data is shown on a linear scale in Figure S3 in the Supporting Information.

Unlike the idealized representation of the gyroid optical metamaterial in Figure 1e, the fabricated metamaterial is not uniformly terminated and exhibits a significant variety of aperiodic surface morphologies (Figure 1a). This arises from the nonuniformity of the electrodeposition growth front during fabrication, as the electrodeposited gold grows spherically outward from randomly distributed nucleation sites at the substrate.[29] We approximate the aperiodic surface morphologies found in the fabricated metamaterial with those periodic surface morphologies exhibited by uniformly terminated gyroid structures. Possible uniform terminations for a ⟨110⟩-oriented gyroid are shown in Figure 1f,g (more terminations are shown in Figure S4 in the Supporting Information). The terminations are characterized by the parameter τ, the distance of the terminating plane from the crystallographic origin in units of structural periodicity in the $[\bar{1}10]$ direction, i.e., $\sqrt{2}a$, with a the gyroid unit cell size. Termination planes separated by $\Delta\tau = 0.5$ are equivalent apart from a shift of the 2D cross-section of the gyroid morphology in the [001] direction (i.e., termination planes are periodic in $\tau = 0.5$ with respect to their optical response).

To highlight the role of different surface terminations on light reflection, reflectance spectra were simulated as a function of termination τ for four different azimuthal angles using the finite-difference time-domain (FDTD) method (**Figure 2**). It is immediately apparent that the simulated reflectance spectra vary significantly both with azimuthal angle and with termination, with the strongest variations found for termination planes in the range $0.1 \lesssim \tau \lesssim 0.3$ (Figure 2a–d). When plotting the reflectance at a single wavelength (650 nm, which will be seen below to capture the response of two important surface morphologies) as a function of termination, a pronounced variation of the linear dichroism with τ is revealed, evidenced here by the absolute difference in reflectance between orthogonal

**ADVANCED
SCIENCE NEWS**

www.advancedsciencenews.com
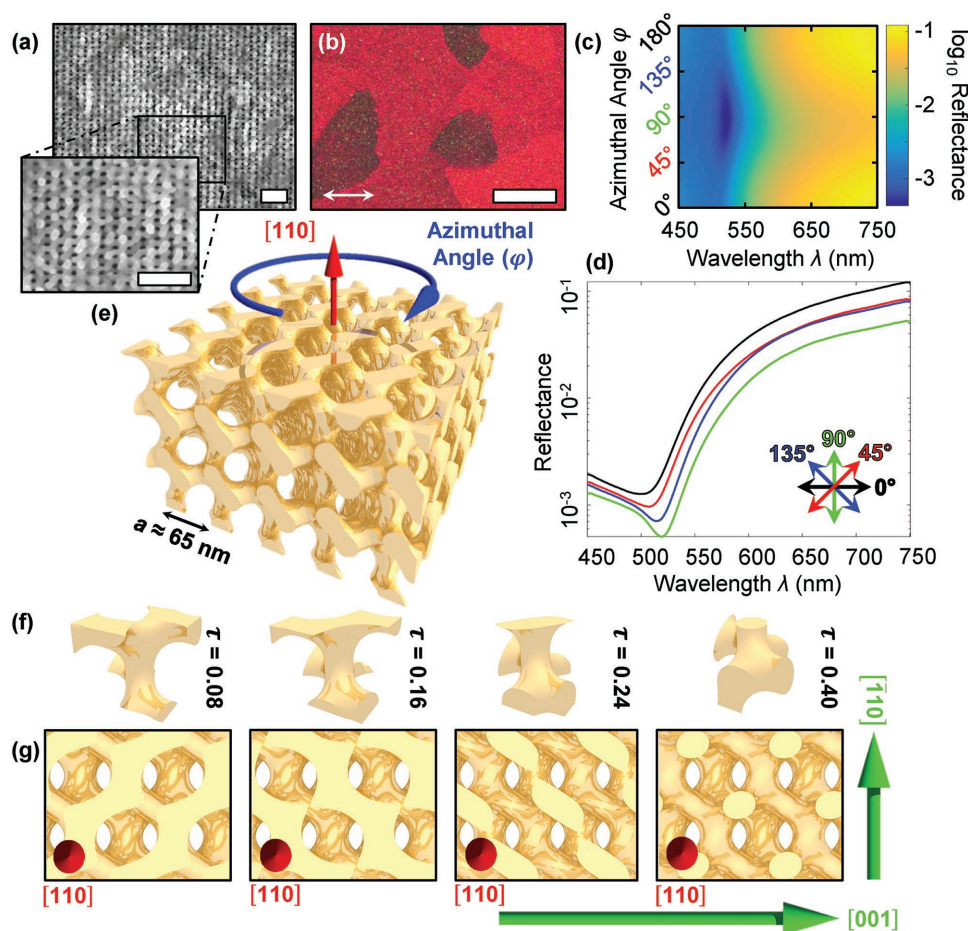
**ADVANCED
MATERIALS**

www.advmat.de

Figure 1. Linear dichroism of gold gyroid optical metamaterials. a) Scanning electron microscopy images of a single-domain gold gyroid. Scale bars: 200 nm. b) Optical reflection microscopy image of several gold gyroid domains with different in-plane orientations. The double-arrow shows the orientation of the polarizer and analyzer. Scale bar: 50 µm. c) Reflectance of linearly polarized light from a single-domain gold gyroid as a function of azimuthal angle and d) at the four azimuthal angles indicated in the inset. The angle φ is defined with respect to the $[\bar{1}10]$ direction of the gyroid. e) Schematic of the single gyroid morphology, highlighting the [110] direction oriented normal to the substrate. f) Four gyroid unit cell elements with surface terminations of $\tau = 0.08$, 0.16, 0.24, and 0.40, where τ is the distance of the terminating plane from the crystallographic origin in units of periodicity in the $[\bar{1}\bar{1}0]$ direction (i.e., $\sqrt{2}a$). g) Surface views of the (110) gyroid plane corresponding to the τ values of (f).

orientations of linearly polarized light (Figure 2e). Clearly, there exists a distinct relationship between surface morphology of the gyroid metamaterial and the observed linear dichroism.

The sharp spectral features in Figure 2 suggest the presence of optical resonances that arise from structurally well-defined surface morphologies. A qualitative comparison of Figure 2e with Figure 1f,g suggests that two distinctive surface morphologies give rise to the marked dichroism observed for the terminations $\tau \approx 0.16$ and 0.24. For the termination plane of $\tau \approx 0.16$, the surface morphology is laterally extended, creating a current pathway in one dimension (arrows in Figure 2e); for the termination plane of $\tau \approx 0.24$, the surface morphology is laterally disconnected. Both surface morphologies also feature small gaps between adjacent disconnected protrusions (circles in Figure 2e) and exhibit protrusions which are only sparsely connected to the bulk gyroid via one vertical strut per repeat unit (Figure 1f). These two distinctive surface morphologies—lateral connectedness (or, conversely, current pathways) and coupled gaps—are able to support the formation of confined

(i.e., nonpropagating) anisotropic plasmonic modes due to their low-connectivity to the underlying bulk morphology.

The underlying physics can thus be understood by analogy to an anisotropic metasurface atop the isotropic bulk gyroid metamaterial. To illustrate this analogy, the gyroid surface at termination $\tau = 0.24$ was modeled as a thin anisotropic effective medium layer (i.e., a metasurface) atop an isotropic semiinfinite bulk (i.e., the metamaterial). A Maxwell–Garnett approach was employed, which accounts for the anisotropy of the surface protrusions (see Materials and Methods in the Supporting Information) but which cannot explicitly account for any coupling between such protrusions. The analytically calculated and simulated reflectance spectra for four azimuthal angles φ are plotted in **Figure 3**a. The permittivities derived from the analytical calculations for the thin anisotropic metasurface and isotropic bulk gyroid metamaterial are shown in Figure 3b,c, respectively. Parallel to the long axis of the anisotropic surface morphology ($\varphi = 55°$), the metasurface exhibits a resonance at $\approx$630 nm (Figure 3b) with a particularly low reflectance at and
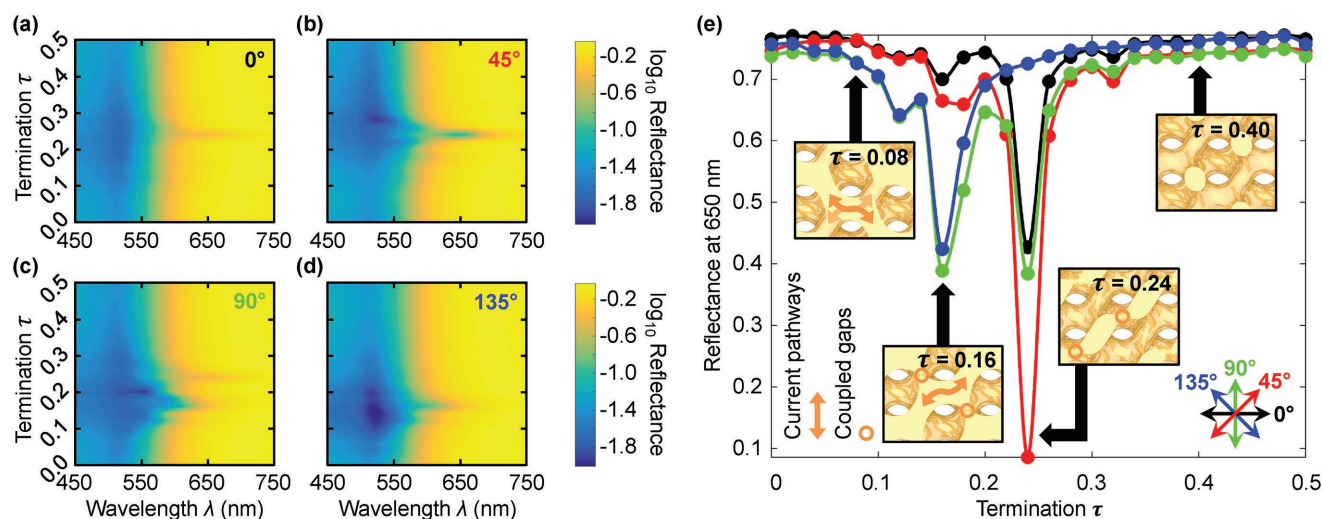
Figure 2. Simulated reflectance spectra and linear dichroism as a function of surface termination. Simulated reflectance spectra as a function of termination τ for azimuthal angles φ of a) 0°, b) 45°, c) 90°, and d) 135°. e) Reflectance at 650 nm as a function of τ for the same φ values, highlighting the continuous current pathways (orange arrows) and coupled gaps (orange circles) of the various gyroid surface morphologies. The angle φ is defined with respect to the [$\bar{1}$10] direction of the gyroid (cf. Figure 1).

above this wavelength (Figure 3a). In contrast, perpendicular to this axis (φ = 145°), the metasurface behaves as a low refractive index dielectric and is therefore almost transparent at normal incidence. The optical response is therefore for this polarization almost entirely that of the underlying bulk gyroid (Figure 3c). The strong correlation between the analytical and numerical calculations implies that the concept of a "metasurface atop a metamaterial" serves as a particularly useful conceptual tool with which the optical properties of uniformly terminated gyroid optical metamaterials can be understood.

To probe the relative importance of the two structural motifs—current pathways and coupled gaps—which lead to resonant behavior, FDTD simulations of only the surface termination layer (i.e., the metasurface layer), without the underlying bulk gyroid, were performed. We systematically alter the surface geometry for the FDTD calculation such that the coupled gap modes are more or less prominent without otherwise substantially altering the anisotropy or periodicity of the structures. The insets in **Figure 4**a,b show the geometry used for the two strongly dichroic terminations: a lateral translation of every second row along φ = 45° for τ = 0.16, and a rotation of the elongated surface features ("islands") around their central axes for τ = 0.24. Figure 4c,d clearly shows how the coupled gap modes, and therefore the overall reflectance spectra, are perturbed by these two modifications, which preserve the topology of the surface protrusions but alter their relative position and orientation. For both terminations, the wavelength at which maximal dichroism occurs is redshifted by ≈90 nm and ≈30 nm for τ = 0.16 and 0.24, respectively. The strength of the linear dichroism (approximated here as the difference between maximal and minimal reflectance at orthogonal linear polarizations) is affected only marginally for τ = 0.16, while it is reduced by ≈0.1 upon the rotation of the islands in the τ = 0.24 case (Figure S6, Supporting Information). This decrease in dichroism is indicative of a coupling of the surface modes across the gaps when the islands are aligned. We note that a

detailed understanding of how the modes identified in this numerical analysis couple with the bulk metamaterial would require further investigation, and will be the subject of a subsequent study.

These simulation results indicate that the reflection spectra are mainly dominated by localized surface plasmons supported by anisotropic protrusions acting as optical nanoantennas (Figure 4). The reflection spectra are, however, considerably perturbed due to the interaction between the laterally periodic nanoantennas, giving rise to strong plasmonic coupling and field enhancement in the gaps between them. The associated redshift is well known and understood.[30] For the two cases where the surface terminations form quasi-1D surface morphologies, these localized surface plasmons lead to a pronounced linear dichroism either perpendicular to the connected pathways (τ = 0.16) or parallel to the long axis of the isolated protrusions (τ = 0.24). This is not the case for non-interacting and near-isotropic isolated protrusions (e.g., τ = 0.4) or for protrusions fully connected laterally in two dimensions (e.g., τ = 0.08). This is illustrated in Figure S5 in the Supporting Information, where the strength of the linear dichroism and the direction of maximal reflectance are plotted versus wavelength and termination. Figure S5 in the Supporting Information provides additional evidence that the linear dichroism arises predominantly from the two terminations τ = 0.16 and 0.24, as suggested by Figure 2e. For these terminations, the linear dichroism is spectrally broad-band, extending from λ ≈ 500 nm into the red. It is most pronounced for τ = 0.24, which is indicative of lateral mode-coupling across the gaps.

Unlike idealized simulations, fabricated gyroid optical metamaterials exhibit a variety of aperiodic surface morphologies (cf. Figure 1a), a subset of which are anticipated to exhibit the approximate spectral response of uniformly terminated gyroid structures explored above. The optical response of the non-uniform fabricated metamaterials is therefore approximated by averaging the simulated reflectance spectra over a range of
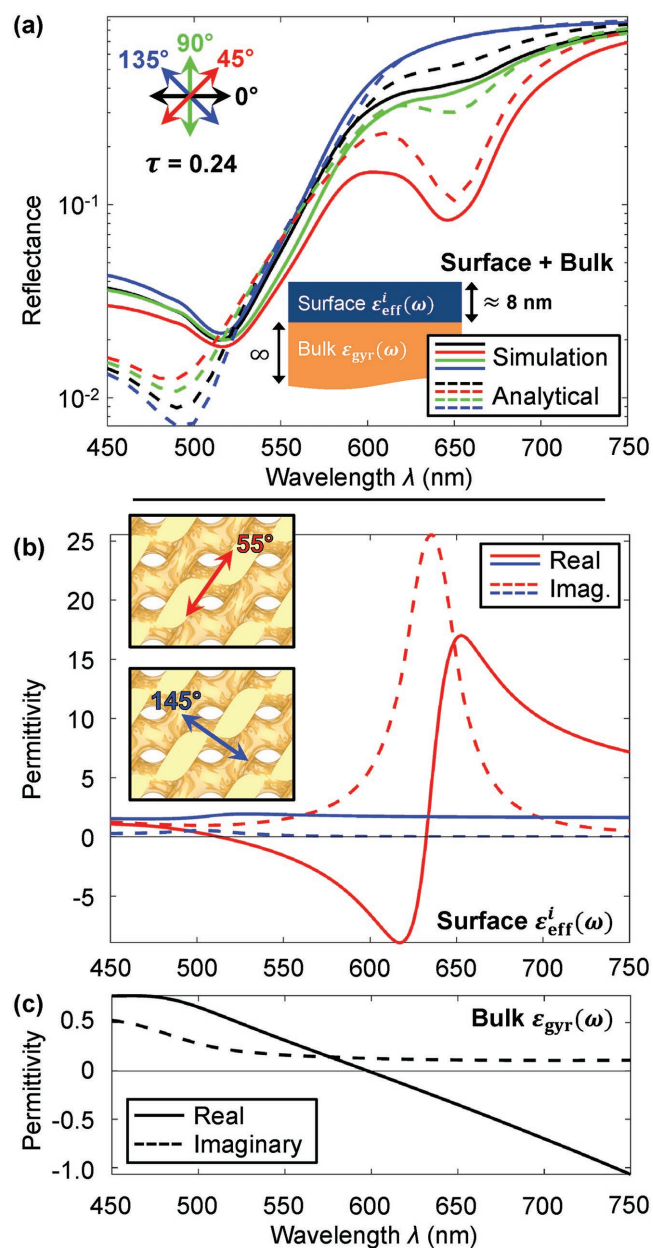
Figure 3. Simulated and analytical reflectance spectra and the calculated permittivities of a Maxwell–Garnett effective medium metasurface and the bulk gyroid metamaterial. a) Simulated (solid lines) and analytical (dashed lines) reflectance spectra at azimuthal angles $\varphi = 0°$ (black), $45°$ (red), $90°$ (green), and $135°$ (blue). b) Real (solid lines) and imaginary (dashed lines) parts of the permittivities of the Maxwell–Garnett effective medium layer parallel ($\varphi = 55°$; red) and perpendicular ($\varphi = 145°$; blue) to the long axis of the effective medium ellipsoidal inclusions (see Materials and Methods in the Supporting Information). c) Real (sold line) and imaginary (dashed line) parts of the permittivity of the bulk gyroid.

termination surfaces. **Figure 5**a,b shows the cases where the terminations are averaged around the two values for which a strong dichroism is observed (i.e., $\tau = 0.16$ and 0.24), in comparison with experimental results. Since the dichroism axis for $\tau = 0.16$ and 0.24 is rotated by $\approx 90°$ (cf. Figure S5 in the Supporting Information), choosing an averaging interval that

crosses the $\tau = 0.2$ boundary significantly diminishes the effective dichroism (Figure 5c). This makes the predicted reflectance very sensitive to the details of the averaging procedure.

Using an appropriate range of terminations, both sets of simulated spectra agree qualitatively with the experimental results. They exhibit a single extinction peak at ≈ 525 nm, a strong linear dichroism, and a similar magnitude of reflectance over the entire wavelength range (Figure 5a). In more detail, however, there are marked differences. For both termination ranges, $\tau = 0.14 \rightarrow 0.18$ and $\tau = 0.22 \rightarrow 0.26$, the simulated dichroism disappears for long wavelengths, while experimentally it extends into the infrared. For $\tau \approx 0.24$, the simulations do not show the dichroism maximum observed at ≈ 520 nm, but rather a shoulder in the 550–650 nm range, substantially underestimating the dichroism between 500 and 550 nm.

Most importantly, however, the polarization angle at which the measured reflectance is maximal is not well matched by the simulations. While the experimentally determined dichroism angle is $\approx 0°$, the two dichroism peaks lie at $\varphi = 45°$ and $135°$, shown in (Figure S5, Supporting Information). As demonstrated in Figure 1c, an overzealous averaging procedure results in a reduction in dichroism rather than in a substantial dichroism at some intermediate angle (e.g., $90°$).

Unsurprisingly, a simple averaging routine of the reflectances of periodic and uniformly terminated gold gyroid surfaces is not sufficient to accurately describe the reflectance of a surface which is instead aperiodic and rough. Such a procedure implicitly assumes that individual surface morphologies exhibit optical properties identical to periodic arrangements of infinite lateral extent, and that there is no coupling between the morphologies characterized by different terminations. In our fabricated metamaterials, however, it is most likely that all these plasmonic surface elements couple, which gives rise to a much richer resonance behavior than is captured in models that ignore such coupling. For example, previous studies have confirmed that the dichroism observed in Figure 1b is indeed correlated with the domain orientation (i.e., the dichroic regions are gyroid domains with different in-plane orientations), which implies a cumulative optical response of the rough gold gyroid surface which cannot readily be modeled with currently available techniques.[13,24] Additionally, a rough gold gyroid surface may present morphologies associated with inclined terminations (i.e., those associated with crystallographic planes other than (110)), which are not considered here.

Based on these results, it is interesting to re-examine results from recent literature. For example, the strength of the dichroism—measured here as the spectral shift of a resonant feature under orthogonal orientations of linearly polarized light—observed by Vignolini et al. (a shift of the extinction peak by ≈ 100 nm),[12] Salvatore et al. (a shift of the "plasma edge" by ≈ 15 nm),[13] and in the present work (a shift of the extinction peak by ≈ 25 nm) are all significantly different despite only small variations in fabrication conditions. A similar variation is observed for the angle of maximal reflectance, which was found at $135°$[12] and $0°$,[13] and the here-presented results relative to the [100] direction. These changes probably arise from small differences in the sample preparation protocols. While these differences might give rise to only minute structural variations on the order of a fraction of the gyroid lattice constant
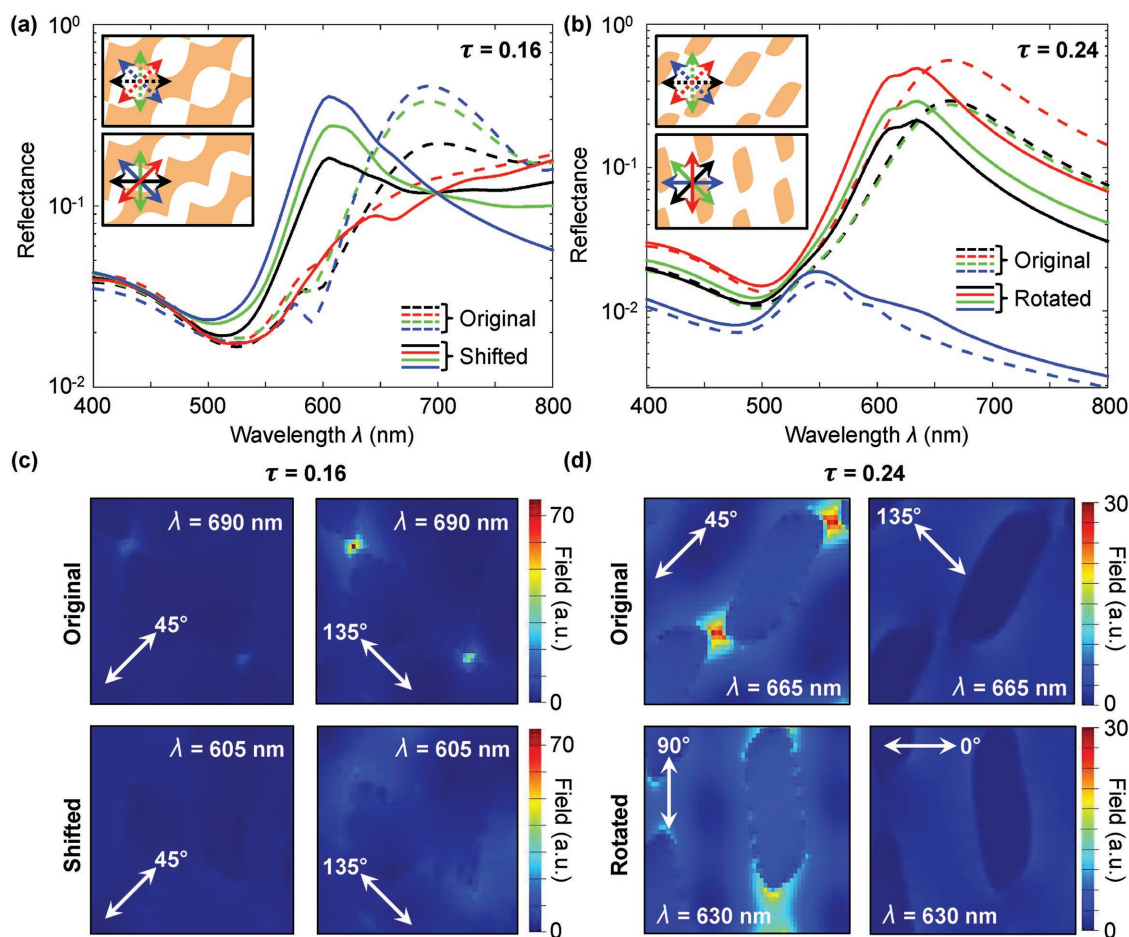
**ADVANCED
SCIENCE NEWS**

www.advancedsciencenews.com

**ADVANCED
MATERIALS**

www.advmat.de

Figure 4. Relative contribution of anisotropic protrusions and coupled gaps to the observed linear dichroism. a,b) Simulated reflectance spectra of an 8 nm thick gold gyroid "metasurface" without the underlying bulk metamaterial at terminations of τ of 0.16 (a) and 0.24 (b). The dashed lines indicate the spectra for four orientations of linearly polarized light of the original surface morphology (i.e., the termination of the bulk gyroid lattice); the solid lines indicate the spectra for altered morphologies whereby neighboring protrusions are shifted (a) or rotated (b) to maintain protrusion shape and orientation (relative to the incident linearly polarized light) but to disrupt coupling between protrusions (insets). c,d) Electric field profiles (magnitude) at maximally resonant wavelengths for terminations τ of 0.16 (c) and 0.24 (d).

(e.g., small differences in filling fraction or the thickness of struts and joints), it is clear from our simulations that even such subtle variations will have a major impact on the reflectance spectra and thereby the dichroism.

The terminations of the gyroid morphology have been characterized by τ, the fractional distance from the crystallographic origin to the terminating surface in units of repeat distance in the $[\overline{1}\overline{1}0]$ direction (i.e., $\sqrt{2}a$). This characterization encodes the length scale over which striking differences in the simulated reflectance spectra are observed. Termination surfaces which exhibit a strong dichroism are separated from those with almost no dichroism by as little as $\Delta\tau \approx 0.06$–5 nm (Figure 2e). This length scale is deeply subwavelength ($\Delta\tau \approx \lambda/100$) and substantially smaller than the unit cell size ($a \approx 65$ nm). The bulk optics of the entire optical metamaterial are therefore sensitive to the existence and morphology of surface features of just a few nanometers.

A number of implications follow from the observation that subwavelength terminations are responsible for the linear dichroism of gyroid optical metamaterials. As the termination

surfaces presented by different orientations of the gyroid differ greatly, so too does the linear dichroism. Gyroid optical metamaterials with the directions ⟨100⟩ and ⟨111⟩ perpendicular to the substrate are highly desirable due to the existence of a circular dichroism in those directions.[12,16,27] It remains to be seen whether a linear dichroism also exists for these orientations of the gyroid morphology.

Furthermore, our results demand a reassessment of the existing literature concerning the linear and circular dichroism of bulk gyroid optical metamaterials (see, e.g., ref. [20], and references therein]). In these publications, the linear dichroism of the gyroid optical metamaterial was characterized with respect to the gyroid lattice orientation. This is, however, only partially correct, since our results show that different surface terminations of the same gyroid lattice orientation give rise to markedly different reflectances and dichroism signatures. In particular, it is possible that slight differences in surface termination across a single gyroid domain will cause a dramatic change in reflectance and hence in the optical appearance of the material. Finally, a similar study is required to explore whether differing terminations of the
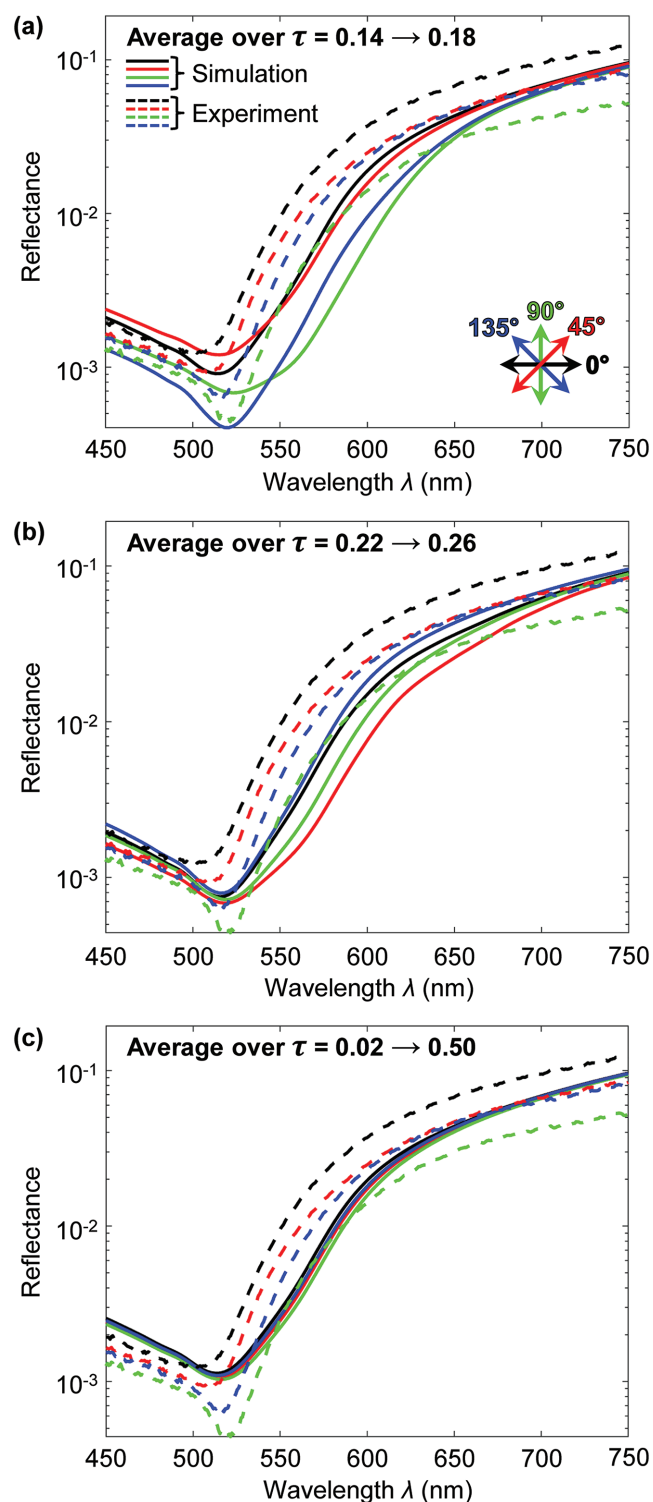
Figure 5. Average simulated reflectance spectra. Simulated (solid lines) and experimental (dashed lines) reflection spectra averaged over termination ranges indicated in the figure. The line colors correspond to the azimuthal angles, defined with respect to the [$\bar{1}10$] direction of the gyroid.

In conclusion, we demonstrate that the terminations of gyroid optical metamaterials induce a pronounced linear dichroism. Terminations break the cubic symmetry of the bulk gyroid morphology, strongly effecting its optical properties. This effect can be considered analogous to that of placing an anisotropic metasurface atop the bulk gyroid metamaterial, whereby the optical properties of the metasurface are determined by the morphology of the terminations.

These findings have significant consequences for all classes of plasmonic metamaterials, whether fabricated "top down" by nanolithography or "bottom up" by polymer self-assembly. While it was previously assumed that the optical properties of these materials are predominantly determined by their bulk morphology, this work demonstrates that this is not the case and that the optical effect of the surface morphology is in fact striking and dependent on sub-5 nm scale features. The extreme sensitivity of these surface effects poses new challenges for the reliable fabrication of plasmonic metamaterials with precisely tailored optical properties. Additionally, this complexity opens the possibility of exploring interesting physics associated with surface states on 3D optical metamaterials, such as Weyl points, pseudo Weyl points, and line nodes.[31–34] Hence, the effect of terminations or similar surface defects in bulk optical metamaterials can lead to fascinating new physics.

Supporting Information

Supporting Information is available from the Wiley Online Library or from the author. Additional data related to this publication is available at the University of Cambridge data repository (http://dx.doi.org/10.17863/CAM.31744).

Acknowledgements

Conflict of Interest

The authors declare no conflict of interest.

Keywords

gyroid morphology give rise to the observed circular dichroism of the gyroid optical metamaterial along the ⟨100⟩ and ⟨111⟩ directions,[12,27] or for other gyroid surface symmetries.

[1] W. Cai, V. Shalaev, *Optical Metamaterials*, Springer, Heidelberg, Germany **2010**.

[2] J. B. Pendry, *Phys. Rev. Lett.* **2000**, *85*, 3966.

[3] J. B. Pendry, D. Schurig, D. R. Smith, *Science* **2011**, *1780*, 1780.

[4] A. Poddubny, I. Iorsh, P. Belov, Y. Kivshar, *Nat. Photonics* **2013**, *7*, 948.

[5] M. Kaniber, K. Schraml, A. Regler, J. Bartl, G. Glashagen, F. Flassig, J. Wierzbowski, J. J. Finley, *Sci. Rep.* **2016**, *6*, 23203.

[6] W. Zhu, K. B. Crozier, *Nat. Commun.* **2014**, *5*, 5228.

[7] Z. Gan, M. D. Turner, M. Gu, *Sci. Adv.* **2016**, *2*, 5.

[8] M. Hentschel, M. Schäferling, X. Duan, H. Giessen, N. Liu, *Sci. Adv.* **2017**, *3*, e1602735.

[9] J. Fischer, M. Wegener, *Laser Photonics Rev.* **2013**, *7*, 22.

[10] A. Boltasseva, V. M. Shalaev, *Metamaterials* **2008**, *2*, 1.

[11] C. M. Soukoulis, M. Wegener, *Nat. Photonics* **2011**, *5*, 523.

[12] S. Vignolini, N. A. Yufa, P. S. Cunha, S. Guldin, I. Rushkin, M. Stefik, K. Hur, U. Wiesner, J. J. Baumberg, U. Steiner, *Adv. Mater.* **2012**, *24*, OP23.

[13] S. Salvatore, A. Demetriadou, S. Vignolini, S. S. Oh, S. Wuestner, N. A. Yufa, M. Stefik, U. Wiesner, J. J. Baumberg, O. Hess, U. Steiner, *Adv. Mater.* **2013**, *25*, 2713.

[14] S. Salvatore, *Optical Metamaterials by Block Copolymer Self-Assembly (Springer Theses)*, Springer, Berlin **2014**.

[15] J. A. Dolan, M. Saba, R. Dehmel, I. Gunkel, Y. Gu, U. Wiesner, O. Hess, T. D. Wilkinson, J. J. Baumberg, U. Steiner, B. D. Wilts, *ACS Photonics* **2016**, *3*, 1888.

[16] K. Hur, Y. Francesato, V. Giannini, S. A. Maier, R. G. Hennig, U. Wiesner, *Angew. Chem., Int. Ed.* **2011**, *50*, 11985.

[17] M. Saba, B. D. Wilts, J. Hielscher, G. E. Schröder-Turk, *Mater. Today:. Proc.* **2014**, *1*, 193.

[18] S. T. Hyde, G. E. Schröder-Turk, *Interface Focus* **2012**, *2*, 529.

[19] G. E. Schröder-Turk, A. Fogden, S. T. Hyde, *Eur. Phys. J. B* **2006**, *54*, 509.

[20] J. A. Dolan, B. D. Wilts, S. Vignolini, J. J. Baumberg, U. Steiner, T. D. Wilkinson, *Adv. Opt. Mater.* **2014**, *3*, 12.

[21] M. Saba, M. Thiel, M. D. Turner, S. T. Hyde, M. Gu, K. Grosse-Brauckmann, D. N. Neshev, K. Mecke, G. E. Schröder-Turk, *Phys. Rev. Lett.* **2011**, *106*, 103902.

[22] M. Saba, M. D. Turner, K. Mecke, M. Gu, G. E. Schröder-Turk, *Phys. Rev. B* **2013**, *88*, 245116.

[23] P. Farah, A. Demetriadou, S. Salvatore, S. Vignolini, M. Stefik, U. Wiesner, O. Hess, U. Steiner, V. K. Valev, J. J. Baumberg, *Phys. Rev. Appl.* **2014**, *2*, 044002.

[24] R. Dehmel, J. A. Dolan, Y. Gu, U. Wiesner, T. D. Wilkinson, J. J. Baumberg, U. Steiner, B. D. Wilts, I. Gunkel, *Macromolecules* **2017**, *50*, 6255.

[25] A. Demetriadou, S. S. Oh, S. Wuestner, O. Hess, *New J. Phys.* **2012**, *14*, 083032.

[26] A. Demetriadou, O. Hess, *Phys. Rev. B* **2013**, *87*, 161101.

[27] S. S. Oh, A. Demetriadou, S. Wuestner, O. Hess, *Adv. Mater.* **2013**, *25*, 612.

[28] J. A. Dolan, K. Korzeb, R. Dehmel, K. C. Gödel, M. Stefik, U. Wiesner, T. D. Wilkinson, J. J. Baumberg, B. D. Wilts, U. Steiner, I. Gunkel, *Small* **2018**, *14*, 1802401.

[29] M. R. J. Scherer, P. M. S. Cunha, U. Steiner, *Adv. Mater.* **2014**, *26*, 2403.

[30] K.-H. Su, Q.-H. Wei, X. Zhang, J. Mock, D. R. Smith, S. Schultz, *Nano Lett.* **2003**, *3*, 1087.

[31] L. Lu, L. Fu, J. D. Joannopoulos, M. Soljac, *Nat. Photonics* **2013**, *7*, 294.

[32] L. Lu, Z. Wang, D. Ye, L. Ran, L. Fu, J. D. Joannopoulos, M. Soljačić, *Science* **2015**, *349*, 622.

[33] M. Saba, J. M. Hamm, J. J. Baumberg, O. Hess, *Phys. Rev. Lett.* **2017**, *119*, 227401.

[34] M. Fruchart, S.-Y. Jeon, K. Hur, V. Cheianov, U. Wiesner, V. Vitelli, *Proc. Natl. Acad. Sci. USA* **2018**, *115*, E3655.

1803478 (8 of 8)